

Magnetic Structure and Two-Dimensional Behavior of  $\text{Rb}_2\text{MnCl}_4$  and  $\text{Cs}_2\text{MnCl}_4$ 

A. Epstein, E. Gurewitz, J. Makovsky, and H. Shaked  
 Nuclear Research Centre-Negev, P. O. B. 9001, Beer-Sheva, Israel  
 (Received 15 May 1970)

A neutron-diffraction study of powder samples of  $\text{Rb}_2\text{MnCl}_4$  and  $\text{Cs}_2\text{MnCl}_4$  was performed. These compounds are paramagnetic at room temperature with  $\text{K}_2\text{NiF}_4$ -type structure ( $D_{4h}^{17}-I4/mmm$ ). It was found that both compounds order antiferromagnetically at  $T_N \sim 55^\circ\text{K}$ . In both compounds the magnetic structure below  $T_N$  is collinear with antiferromagnetic axis parallel to  $z$ , isomorphic with that of low-temperature  $\text{K}_2\text{NiF}_4$  ( $F_A m' m' m$ ). Calculations of the dipolar energy show that  $z$  is indeed a direction of lower dipolar energy than  $x$ . In addition, the diffraction patterns exhibit a "ridge" — a broad reflection below about  $180^\circ\text{K}$  which indicates the existence of two-dimensional spin correlations. Such correlations in the planes parallel to (001) are expected and have already been found in  $\text{K}_2\text{NiF}_4$  and isomorphic compounds.

## I. INTRODUCTION

The compounds  $A_2\text{MnCl}_4$  ( $A = \text{Rb}, \text{Cs}$ ) are isostructural to  $\text{K}_2\text{NiF}_4$ .<sup>1</sup> This structure belongs to the tetragonal space group  $D_{4h}^{17}-I4/mmm$  with two molecules per unit cell [Fig. 1(a)]. The compound  $\text{K}_2\text{NiF}_4$  orders antiferromagnetically ( $T_N \sim 97^\circ\text{K}$ ) in a magnetic unit cell with four molecules per cell<sup>2</sup> [Fig. 1(b)]. Above the transition temperature, neutron diffraction from this compound exhibits two-dimensional magnetic critical scattering,<sup>3</sup> which has been the subject of extensive experimental and theoretical studies.<sup>4</sup> We report here the results of a neutron-diffraction study of powder samples of  $\text{Rb}_2\text{MnCl}_4$  and  $\text{Cs}_2\text{MnCl}_4$ . We have found that, as the sample's temperature is lowered below  $180^\circ\text{K}$ , the diffraction patterns of both compounds exhibit a "ridge"<sup>3</sup> characteristic of the two-dimensional antiferromagnet (see Sec. V). At  $57$  and  $52^\circ\text{K}$ ,  $\text{Rb}_2\text{MnCl}_4$  and  $\text{Cs}_2\text{MnCl}_4$ , respectively, order antiferromagnetically in three dimensions in identical magnetic structures. This structure belongs to the magnetic space group  $F_A m' m' m$  and is identical with the magnetic structure of some of the other  $\text{K}_2\text{NiF}_4$ -type compounds.<sup>5,6</sup>

## II. PREPARATION AND CRYSTALLOGRAPHY

The two compounds were prepared according to the following procedure: Stoichiometric amounts of anhydrous  $\text{MnCl}_2$  and  $A\text{Cl}$  ( $A = \text{Rb}, \text{Cs}$ ) were mixed in quartz ampoules. The ampoules were then evacuated and sealed. The published<sup>7</sup> value of the incongruent melting point of  $\text{Rb}_2\text{MnCl}_4$  is  $462^\circ\text{C}$  and that of the congruent melting point of  $\text{Cs}_2\text{MnCl}_4$  is  $538^\circ\text{C}$ . The ampoules were then heated to about  $100^\circ\text{C}$  above the respective melting points. After being kept at this temperature for several hours, the ampoules were slowly cooled to room temperature. An x-ray powder diagram of  $\text{Rb}_2\text{MnCl}_4$  also included very weak  $\text{RbCl}$  lines

and two very faint unidentified lines possibly of  $\text{Rb}_3\text{Mn}_2\text{Cl}_7$ . The  $\text{Cs}_2\text{MnCl}_4$  diagram showed no lines other than those of the pure compound. The chemical unit cell of these  $A_2\text{BX}_4$  compounds is shown in Fig. 1(a). Half of the ionic positions in this cell are as follows:

$$A^+ \text{ at } 4e: \pm(0, 0, z_A),$$

$$B^{++} \text{ at } 2a: (0, 0, 0),$$

$$X_1^- \text{ at } 4c: (0, \frac{1}{2}, 0) \text{ and } (\frac{1}{2}, 0, 0),$$

$$X_{11}^- \text{ at } 4e: \pm(0, 0, z_x).$$

The other half is obtained by applying the body-center translation  $(\frac{1}{2}, \frac{1}{2}, \frac{1}{2})$  to these positions. The unit-cell dimensions of  $\text{Rb}_2\text{MnCl}_4$  were reported by Seifert *et al.*<sup>8</sup> to be  $a = 5.05 \text{ \AA}$  and  $c = 16.18 \text{ \AA}$ . Our neutron-diffraction results (Fig. 2) are in agreement with these values. The unit-cell dimensions of  $\text{Cs}_2\text{MnCl}_4$  were determined from our neutron-diffraction patterns (Fig. 2) to be  $a = 5.15 \text{ \AA}$  and  $c = 17.0 \text{ \AA}$ . A least-squares refinement of the

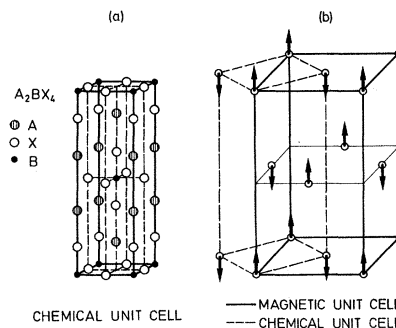


FIG. 1. (a) Chemical unit cell of the  $\text{K}_2\text{NiF}_4$ -type structure. (b) Relation between the magnetic unit cell (solid lines) and the chemical unit cell (dashed lines) of  $A_2\text{MnCl}_4$  ( $A = \text{Rb}, \text{Cs}$ ). The spin structure is also shown.

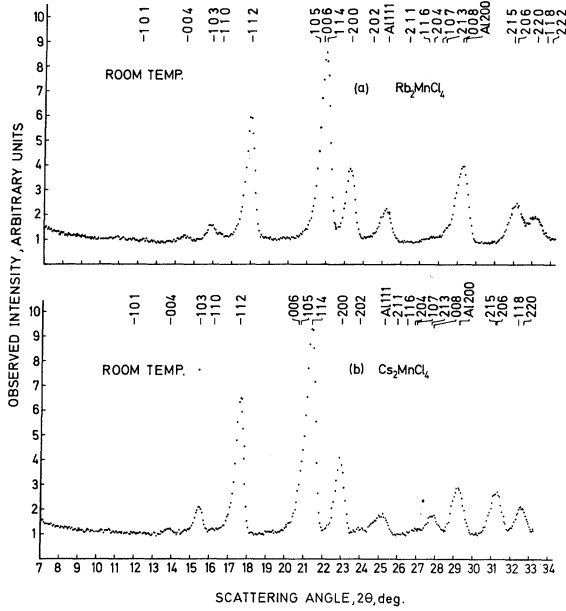


FIG. 2. Neutron ( $\lambda \sim 1.021 \text{ \AA}$ ) diffraction pattern of (a)  $\text{Rb}_2\text{MnCl}_4$  and (b)  $\text{Cs}_2\text{MnCl}_4$  at room temperature. Lines are indexed according to the chemical unit cell.

calculated integrated intensities of eight nuclear reflections was performed. The  $z_{\text{Cl}}$  and  $z_{\text{A}}$  ( $\text{A} = \text{Cs, Rb}$ ) values subsequently found are within 5% of their ideal positions [Fig. 1(a)] on the perovskite-like cube ( $z_{\text{Cl}} = a/2c$ ,  $z_{\text{A}} = \frac{1}{2} - z_{\text{Cl}}$ ; that is, for  $c/a \sim 3.3$ , one has  $z_{\text{Cl}} \sim 0.15$  and  $z_{\text{A}} \sim 0.35$ ).

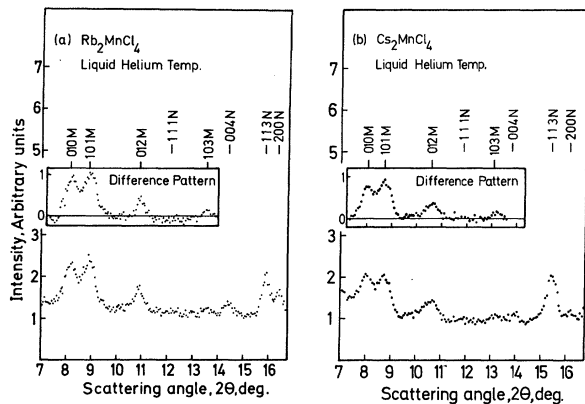


FIG. 3. Neutron-diffraction pattern at liquid-helium temperature of (a)  $\text{Rb}_2\text{MnCl}_4$  ( $\lambda \sim 1.016 \text{ \AA}$ , U. S. -1 diffractometer) and (b)  $\text{Cs}_2\text{MnCl}_4$  ( $\lambda \sim 1.021 \text{ \AA}$ , KANDI diffractometer). Magnetic ( $M$ ) and nuclear ( $N$ ) lines are indexed according to the magnetic ( $F_B$ ) unit cell. The difference between room- and liquid-helium-temperature patterns is also given.

### III. MAGNETIC STRUCTURE AT LIQUID-HELIUM TEMPERATURE

Four magnetic lines appeared in the diffraction patterns of  $\text{Rb}_2\text{MnCl}_4$  and  $\text{Cs}_2\text{MnCl}_4$  at liquid-helium temperature (Fig. 3). On the basis of the  $C$  (chemical) unit cell [Fig. 1(a)], these lines are indexed as  $(\frac{1}{2} \frac{1}{2} 0)$ ,  $(\frac{1}{2} \frac{1}{2} 1)$ ,  $(\frac{1}{2} \frac{1}{2} 2)$ , and  $(\frac{1}{2} \frac{1}{2} 3)$ . The smallest  $M$  (magnetic) unit cell for which the Miller indices of these lines are integers is given by

$$\vec{a}_M = \vec{a}_C + \vec{b}_C, \quad \vec{b}_M = \vec{a}_C - \vec{b}_C, \quad \vec{c}_M = \vec{c}_C.$$

The  $M$  unit cell and its relation to the  $C$  unit cell are shown in Fig. 1(b). The volume ratio of the  $M$ -to- $C$  unit cells is 2. The four observed magnetic lines are indexed on the basis of the  $M$  unit cell as

either (010), (101), (012), and (103)

or (100), (011), (102), and (013).

The magnetic lattices for which these lines are allowed are

either  $F_B$  (generators):  $(0 \frac{1}{2} \frac{1}{2}) \times R$ ,  $(\frac{1}{2} 0 \frac{1}{2})$ ,  $(\frac{1}{2} \frac{1}{2} 0) \times R$ ,

or  $F_A$  (generators):  $(0 \frac{1}{2} \frac{1}{2})$ ,  $(\frac{1}{2} 0 \frac{1}{2}) \times R$ ,  $(\frac{1}{2} \frac{1}{2} 0) \times R$ ,

respectively. The generators are given in fractions of the  $M$  unit-cell translations and  $R$  is the time-inversion operation. The spin direction is determined from the intensity data (Table I) to be in the  $z$  direction. It was shown by Keffer<sup>10</sup> that the dipolar energy term in the anisotropy energy is the dominant one in the case of  $\text{Mn}^{2+}$  ions in  $\text{MnF}_2$ . In this connection, we have computed the dipolar interaction energy of one ion with about 1000 neighbors. Using  $c/a = 3.3$ , we obtained for the  $F_X$  ( $X = A, B$ ) lattice with spins parallel and perpendicular to the  $z$  direction:

$$E_{\parallel} = -2.638 \mu^2 / a^3, \quad E_{\perp} = 1.319 \mu^2 / a^3.$$

In the two compounds ( $a \sim 5 \text{ \AA}$ ,  $\mu \sim 5 \mu_B$ ) this corresponds to an anisotropy of  $10^{-16}$  erg/ion in the dipolar energy. It is therefore possible that it is

TABLE I. Comparison of the observed and calculated integrated intensities of the magnetic reflections for  $\text{Cs}_2\text{MnCl}_4$ .<sup>a</sup>

$hkl$	Observed	Calculated <sup>b</sup>		
		$x$	$y$	$z$
010	3226	3749	0	3105
101	4476	960	6140	4337
012	1804	3889	1630	1855
103	494	1402	2230	703

<sup>a</sup>Similar results were obtained with  $\text{Rb}_2\text{MnCl}_4$ .

<sup>b</sup>Calculated for  $F_B$  lattice with spins in the  $x$ ,  $y$ , and  $z$  directions with experimental form factor (Ref. 9).

the dipolar energy which causes the spins to align in the  $z$  direction. It is interesting to note that the equality  $E_{\parallel} = -2E_{\perp}$  is also obtained if one considers interactions within the plane (001) only as follows: The dipole-dipole interaction of two collinear spins  $S$  and  $S_j$  is equal (disregarding sign) to  $[1 - 3 \cos^2(\mathbf{r}_j \cdot \mathbf{S})]S^2/r_j^3$ . The average value of  $\cos^2(\mathbf{r}_j \cdot \mathbf{S})$  for all the spins equidistant to  $S$  is  $\frac{1}{2}$  when the spins are perpendicular to  $c$  and 0 when they are parallel to  $c$ , leading to  $E_{\parallel} = -2E_{\perp}$ .

The magnetic space group which corresponds to the structure is

$$\text{either } F_B m' m' m' \\ \text{or } F_A m' m' m'.$$

To each space group belong two spin structures, a structure and its time conjugate, altogether four spin structures. These four spin structures transform into one another under the factor group

$$(F4/mmm1')/(F_X m' m' m')$$

with  $X=A, B$ . The space groups  $F4/mmm1'$  and  $I4/mmm1'$  are identical and refer to the  $M$  and  $C$  unit-cell translations, respectively. The order of this factor group is four and the spin structures represent, therefore, the four possible magnetic domains which are indistinguishable in the powder diffraction.

The magnetic moments calculated from the ratios of magnetic to nuclear reflections are 4.9 and 4.4

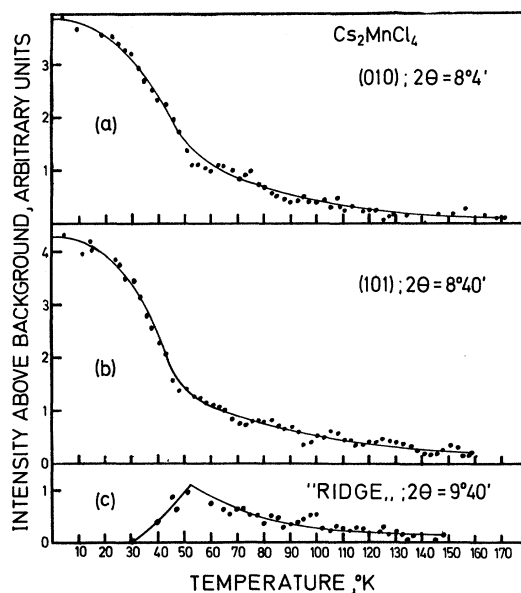


FIG. 4. Temperature dependence of the  $\text{Cs}_2\text{MnCl}_4$  magnetic reflections (a) (010) and (b) (101) and of the (c) "ridge" taken at  $2\theta = 9^\circ 40'$ .

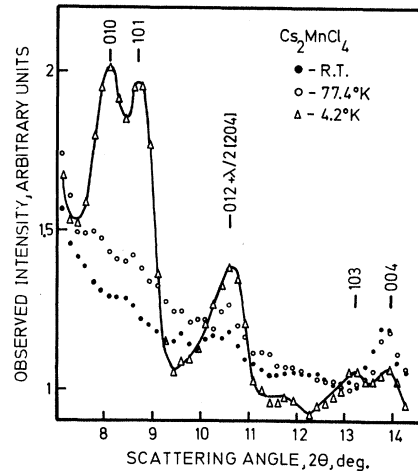


FIG. 5. The  $\text{Cs}_2\text{MnCl}_4$  low-angle diffraction pattern at room, liquid-nitrogen, and liquid-helium temperature.

$\mu_B$  for  $\text{Cs}_2\text{MnCl}_4$  and  $\text{Rb}_2\text{MnCl}_4$ , respectively.

#### IV. MAGNETIC BEHAVIOR ABOVE LIQUID-HELIUM TEMPERATURE

As temperature is increased above 4.2°K, the intensity of neutrons scattered from the magnetic reflections in  $\text{Cs}_2\text{MnCl}_4$  decreases with a progressively increasing slope up to about 55°K [Figs. 4(a) and 4(b)]. At 55°K there is still some residual intensity of (probably) magnetic scattering, which falls with a progressively decreasing slope as temperature is further increased, reaching background at about 180°K. In Fig. 4(c) we show the temperature dependence of the neutron intensity at a position slightly higher than the Bragg angle. As temperature is increased, at about 30°K, some intensity above background appears, increasing with temperature to a maximum at about 55°K and slowly decreasing thereafter, reaching background at about 180°K. In Fig. 5, it is shown that this intensity is a part of a "ridge" which starts at the angle of the lowest-angle magnetic reflection and disappears at large angles. Similar results were obtained with  $\text{Rb}_2\text{MnCl}_4$ . The (010) and (101) magnetic reflections in  $\text{Rb}_2\text{MnCl}_4$  are shown at several temperatures in Fig. 6: As temperature is increased, the two peaks degenerate into a broad ridge.

#### V. DISCUSSION

The residual intensity of the magnetic reflections above the transition temperature is characteristic of some residual magnetic order. Such an effect has already been observed in  $\text{K}_2\text{NiF}_4$ <sup>2,3</sup> and other isostructural compounds<sup>11</sup> and has been interpreted<sup>3</sup> to be a result of long-range two-dimensional spin correlations in the planes parallel to (001). It can be argued that such a magnetic system is indeed

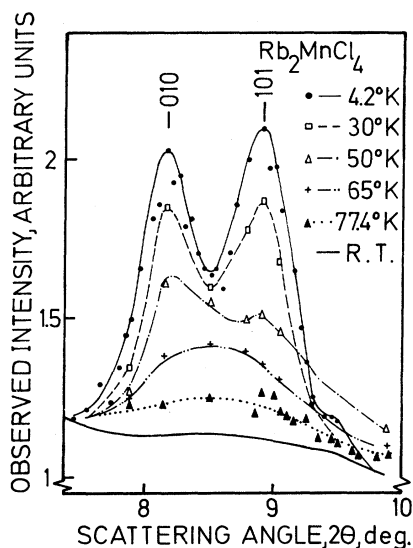


FIG. 6. The  $\text{Rb}_2\text{MnCl}_4$  reflections (010) and (101) at various temperatures between liquid-helium and room temperature.

expected in this type of structure as follows: The magnetic lattice has the property that the vector sum of spins in one (001) plane which are equidistant to a lattice point at an adjacent plane vanishes for all lattice points. The magnetic lattice can be, therefore, subdivided into two equivalent noninteracting sublattices. These sublattices transform into one another under  $(\frac{1}{2}, 0, \frac{1}{2})$  and  $(0, \frac{1}{2}, \frac{1}{2}) \times R$  translations in  $F_B$  or  $(\frac{1}{2}, 0, \frac{1}{2}) \times R$  and  $(0, \frac{1}{2}, \frac{1}{2})$  translations in  $F_A$ . Within each lattice the distance to the first

neighbors on the adjacent plane is more than  $3\sqrt{2}$  times larger than the distance to the first neighbors within the plane. It is therefore expected that interplane interactions are by at least three to four orders of magnitude smaller than the intraplane exchange.<sup>12</sup> As the temperature is lowered below 200 °K, spin correlations appear within every (001) plane with no order between the planes. So to speak, the  $c$  dimension of the magnetic cell is very large, and the reciprocal lattice points are therefore crowded in this direction. Consequently, in the powder pattern, magnetic reflections will appear at all scattering angles above the lowest magnetic scattering angle [(100) reflection in our case]. These reflections give rise to the ridge observed at liquid-nitrogen temperature (Figs. 5 and 6). The height of this ridge decreases with scattering angle due to the Lorentz and magnetic form factors. As the temperature further decreases, the range of correlations within the planes increases, and so does the ridge height (Fig. 4), until a temperature is reached where a three-dimensional order sets in. As the temperature is further lowered, the three-dimensional order builds up, as indicated by the decreasing ridge height [Fig. 4(c)] on one hand, and the increasing height of the magnetic reflections (010) and (101) [Figs. 4(a) and 4(b)] on the other.

#### ACKNOWLEDGMENTS

The authors are indebted to Professor S. Shtrikman of the Weizmann Institute of Science for his kind criticism and suggestions, and to M. Melamud and T. Kulum of the Nuclear Research Centre-Negev for their helpful assistance.

<sup>1</sup>D. Balz and K. Plieth, *Z. Elektrochem.* **59**, 545 (1955).

<sup>2</sup>R. Plumier and E. Legrand, *J. Phys. Radium* **23**, 474 (1962); E. Legrand and R. Plumier, *Phys. Status Solidi* **2**, 317 (1962).

<sup>3</sup>R. J. Birgeneau, J. H. Guggenheim, and G. Shirane, *Phys. Rev. Letters* **22**, 720 (1969).

<sup>4</sup>M. E. Lines, *J. Appl. Phys.* **40**, 1352 (1969).

<sup>5</sup>R. J. Birgeneau, H. J. Guggenheim, and G. Shirane, *Phys. Rev. B* **1**, 2211 (1970).

<sup>6</sup>E. Legrand and M. Verschuere, *J. Phys. Radium* **25**, 578 (1964). These authors have already proposed

this structure for  $\text{Cs}_2\text{MnCl}_4$  on the basis of preliminary results.

<sup>7</sup>P. Ehrlich, F. W. Koknat, and H. J. Siefert, *Z. Anorg. Allgem. Chem.* **341**, 281 (1965).

<sup>8</sup>H. J. Seifert and F. W. Koknat, *Z. Anorg. Allgem. Chem.* **341**, 269 (1965).

<sup>9</sup>G. E. Bacon, *Neutron Diffraction* (Oxford U. P., Oxford, England, 1962).

<sup>10</sup>F. Keffer, *Phys. Rev.* **87**, 608 (1952).

<sup>11</sup>E. Legrand and A. Van den Bosch, *Solid State Commun.* **7**, 1191 (1969).

<sup>12</sup>M. E. Lines, *Phys. Rev.* **164**, 736 (1967).